Defence Science Journal, Vol. 75, No. 5, September 2025, pp. 622-628, DOI : 10.14429/dsj.20578


# Analysis of Failure of Pin Locator for Internal Nose Cap of a Long Range Cruise Missile

M. Sai Madhav* and Manish Roy

*DRDO-Defence Metallurgical Research Laboratory, Hyderabad: 500 058, India*
**E-mail: saimadhav.dmrl@gov.in*

**ABSTRACT**

A steel pin used as a locator for internal nose cap of long range cruise missile was found in cracked condition after it was subjected to transportation, vibration and bump tests. Metallurgical investigation was carried out with the failed pin. The crack was found to be inter-granular and a thin black oxide layer was observed on the fracture surface. Based on the evidence, it is concluded that the pin failed because of quench cracking and the crack was initiated prior to tempering and zinc plating.

**Keywords:** Steel pin; Intergranular; Zinc plating; Quench cracks; Oxide scale; Overload fracture features

## 1. INTRODUCTION

A cruise missile is one which flies at approximately constant speed. It can be a guided missile targeted against terrestrial or naval components. These missiles are capable of delivering a large war head with extreme precision over large distances. Modern cruise missiles can travel at high subsonic, supersonic, or hypersonic speeds. They can navigate on their own and can fly on a low-altitude trajectory. Cruise missiles can be classified based on their size, speed, range, launching platforms and guidance systems. Launching platforms can be air, submarine or ship. The guidance systems can be satellite or inertial navigation such as TERCOM etc. Nuclear or conventional warhead can be carried by large cruise missiles. In contrast, only conventional warheads can be carried by smaller ones.

Pins are part of various engineering applications. Failure analysis of various pins of different systems is reported in the literature[1-9]. Papadopoulou[1], *et al.*. investigated failure of pins of a chain assembly made of steel and this assembly is a part of a continuous cold drawing machine and noted multiple-origin rotating bending fatigue initiated from the pin circumference as a result of tensile and/or bending stresses is responsible for failure. According to Javidinejad[2] the failure occurs earlier than expected because of higher stress levels in the partial length un-symmetric pin clevis configuration. The formation of quench crack was attributed to the failure of a twist lock pin supporting one side of two stacked shipping containers by Kral[3], *et al.*. Observation of Xu and Yu[4] indicates that the surface region of the internal hole was decarburized and this results in reduction of the fatigue strength. This resulted in failure of diesel engine piston-pin used in a truck. High notch effect and the incorrect mounting of the specimens were found to be the reason for failure of a mandrel pin mounted on a rolling contact test bench by Solazzi[5], *et al.*. As reported by Pepi, and Wechsler[6], Rolling Contact Fatigue (RCF) is mainly responsible for the failure of the hinge pin (HHP) assembly which was horizontal from an cargo helicopter of Army. Slabbert[7], *et al.* found that conveyor chain pins of a sugar plant cracked because of hydrogen embrittlement. Hydrogen embrittlement was also responsible for the damage of chain anchor pins on a fork lift truck as revealed by Ifezue and Tobins[8]. Jha[9], *et al.* carried out metallurgical examination of a shear pin employed to disengage the rotor installed in a vertical mixer for mixing solid propellant of satellite launching vehicle and reported that presence of inclusions located close to the notch in the steel caused initiation of fatigue crack.

A steel pin used as a locator for internal nose cap of long range cruise missile was found to have a crack along the longitudinal axis. It is informed that 12 mm dia rod was heat treated by austenitizing at 900-930 °C for 60-75 min. followed by water quenching and then tempering at 480-520 °C for 60-75 min. followed by air cooling. The heat treated rod was machined by threading, hexagon cutting etc. to finish to product dimensions as per drawing. The finished pin was subjected to zinc plating followed by baking treatment to remove entrapped hydrogen at 195 °C for 10 hrs. The finished component was assembled in the system and subjected to transportation, vibration and bump tests. After the tests and during visual examination, a crack along the length of the pin was observed. To confirm the crack, magnetic particle inspection was carried out on the pin. Alignment of particles was observed along the crack length.

In view of the above literature and fact, the cracked steel pin was examined for identification of cause for the formation of the crack. A comprehensive metallurgical investigation was carried out and the results are presented in the in details in this work.

Received : 04 September 2024, Revised : 16 March 2025
Accepted : 22 May 2025, Online published : 01 September 2025

## 2. INVESTIGATION AND RESULTS

### 2.1 Visual Examination

The cracked pin in the as-received condition is shown in Fig.1. Visual observation has indicated a crack from the junction of the hexagonal portion and the thread grove and to a length equal to the thread portion of the pin. No crack was observed in the hexagonal portion as well as the cylindrical portions of the pin.

**Figure 1. As received condition of the cracked pin.**

### 2.2 Stereographic Examination

Stereo examination has displayed that the crack is present from the end of the hexagonal portion and the first thread joining position to the end of the last thread. It is to be noted that no crack was observed on the hexagonal portion as well as on the cylindrical portion of the pin. The centre portion with the crack is illustrated in Fig. 2.

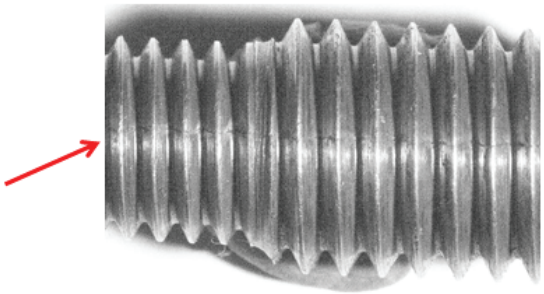

**Figure 2. Stereo microscopic images of pin showing crack.**

### 2.3 Metallography

Sections of the failed components were prepared for metallographic examination and observed under optical microscope. The microstructure of the pin was seen on longitudinal directions. The etching reagent was Villella's reagent. The microstructure provided in Fig. 3 reveals tempered martensite structure.

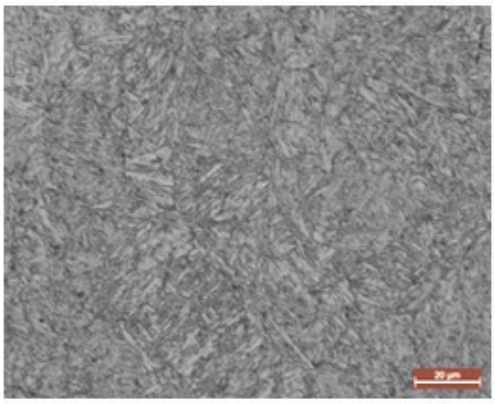

**Figure 3. Photomicro graph of the pin in longitudinal direction showing tempered martensite structure. Etchant Villella's Reagent.**

### 2.4 Chemical Analysis

X-ray florescence spectroscopy (XRF), inductively coupled plasma optical emission spectrophotometer (ICP-OES) employed to carry out elemental analysis of the failed component. LECO oxygen, nitrogen analyser was used for detection of the interstitial elements. The measured composition of the pin is listed in Table 1. It is clear that all parts are iron based.

**Table 1. Measured composition of the pin**

| Element | C | Cr | Mn | Fe. |
|---|---|---|---|---|
| wt % | 0.3 ± 0.05 | 1.0 ± 0.3 | 1.0 ± 0.2 | Bal. |

### 2.5 Hardness

Vickers hardness was measured on the sample using universal hardness tester at a load of 20 Kg. Average Vickers hardness of the pin was found to be 349 HV.

### 2.6 Examination of Damaged Surfaces

The defective pin was cut cross-sectional as per schematic presented in Fig. 4 and viewed under optical microscope. The optical micrograph shown in Fig. 5(a) reveals that the crack has propagated to a depth of 1/3$^{rd}$ of the diameter of the rod. The cut surface was polished and examined under optical microscopy. The optical image is given in Fig. 5(b). Figure 5(b) indicates a crack that had propagated in a zigzag pattern. To open the crack for fracture surface examination, the cross section portion with the crack was cut perpendicular to the depth of the crack along the length. After cutting across the crack length, the two mating surfaces of the crack were opened by a small amount of force and by giving a slot into the crack. The mating surfaces of the crack are shown in Fig. 6. The entire crack has shown dark black coloured surface except the force opened region which is bright.

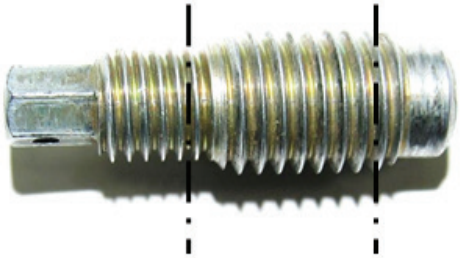

**Figure 4. Schematic showing the cutting of the pin. The portion between the lines was viewed under microscope.**

The low magnification SEM fractographs showing the fracture surface from the thread portion to the about 90 % of the fracture surface is illustrated in Fig. 7(a) through Fig. 7(d). The remaining portion showing the cut marks is the force opened region. Near the threaded portion a coating was observed along the contour of the thread while the fracture surface is covered by a thick oxide scale (Fig. 7(b)). Deep into the fracture surface intergranular fracture features covered by oxide scale was observed (Fig. 7(c)). At the junction of the fracture surface and the force opened region, rubbed fracture features and overload fracture features were observed (Fig.7(d)).

Optical micrograph given in Fig. 8(a) shows the zigzag pattern of the crack. The area near the crack surface has

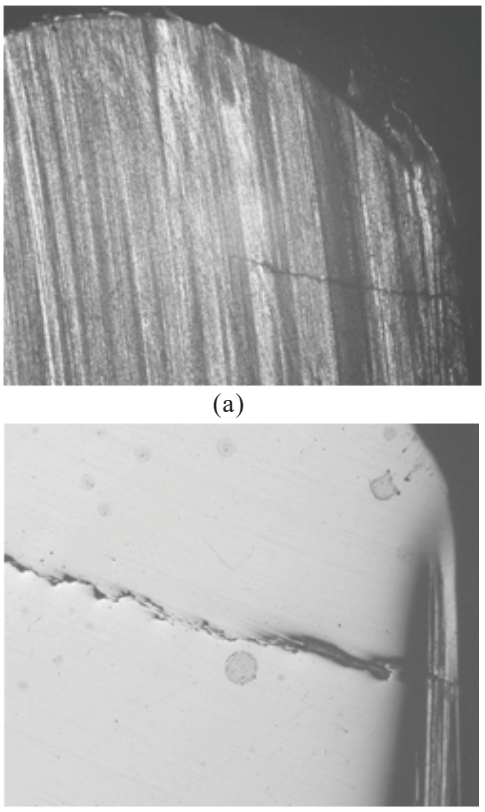

(a) (b)

**Figure 5. (a) Optical micrograph showing crack in as cut surface; and (b) Optical micrograph showing crack after polishing.**

**Figure 6. Photograph showing the two mating surfaces of the crack after cutting.**

revealed cracking along the grain boundaries as seen in Fig. 8(b). EDAX analysis was carried out on the coating of the thread has shown the presence of zinc in addition to matrix elements as given in Fig. 9(a). EDAX analysis on the fracture surface of the threads and on the intergranular region has also revealed the presence of zinc in association with matrix elements with the same intensity as on the coating region. On the other hand the forced opened region has revealed only the matrix elements in EDAX analysis. No traces of Zinc are seen in this region as can be seen from Fig. 9(b).

### 2.7 Numerical Simulations

A 2D finite element model coupled with field element having a total of 9,000 nodes and 7,000 elements in ANSYS 13.0 is developed for the given geometry. This is a comprehensive Computer-Aided Engineering (CAE) software, to simulate, analyze, and optimize stress distribution across various domains. Mesh refinement is found to be adequate as less than

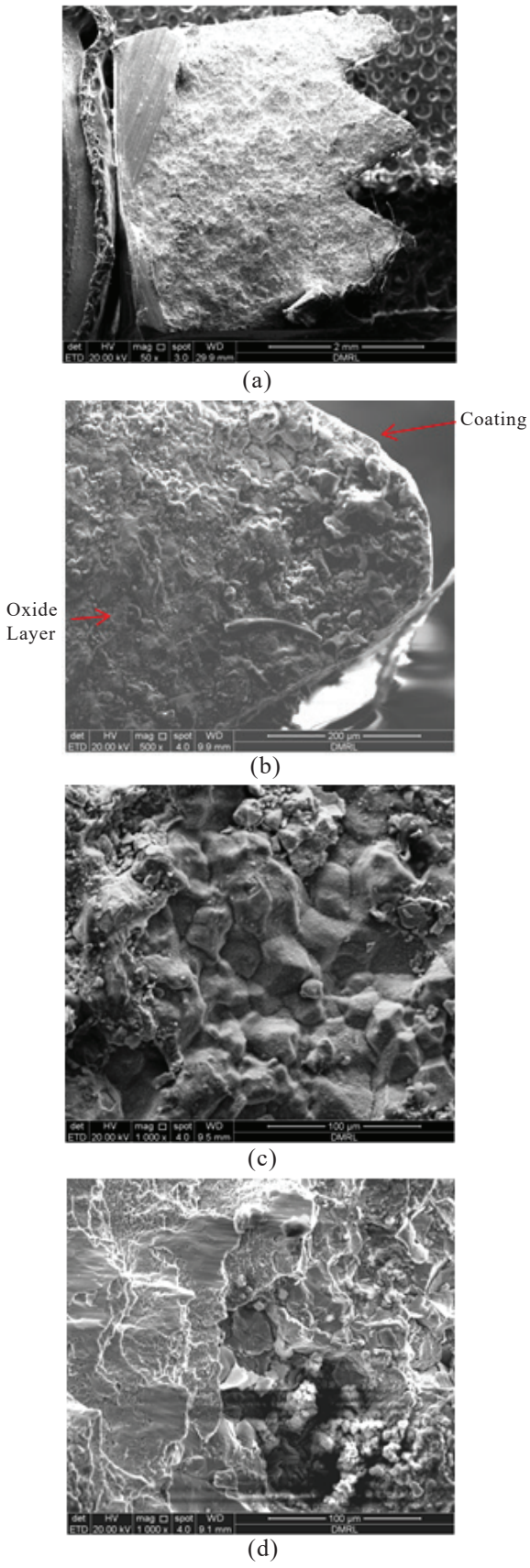


(a) (b) (c) (d)

**Figure 7. (a) SEM fractograph showing fracture surfaces; (b) SEM fractograph showing fracture surface with coating and oxide layer; (c) SEM fractograph showing intergranular fracture surface; (d) SEM fractograph showing rubbing and overload fracture surface.**

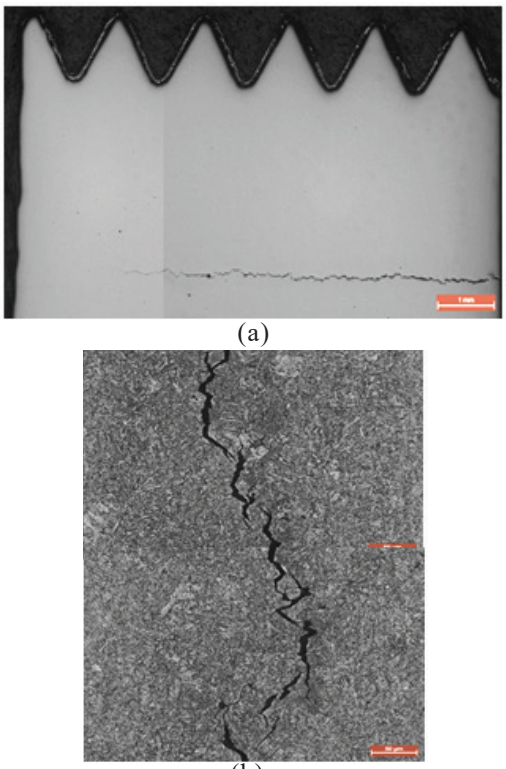

(a)

(b)

**Figure 9. (a) Optical photomicrographs showing the zig-zag pattern of the crack in unetched condition; and (b) Optical photomicrographs showing the zig-zag pattern of the crack in of the crack after etching.**

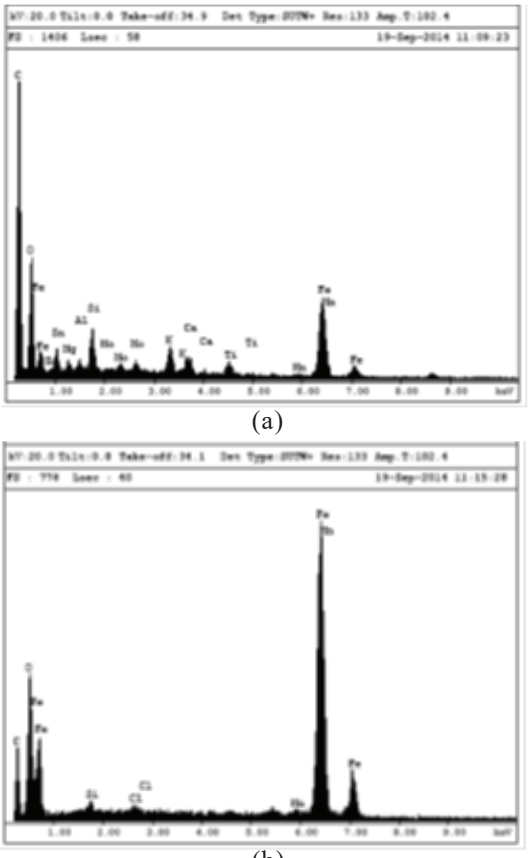

(a)

(b)

**Figure 9. (a) EDAX analysis of fracture surface on the teeth showing presence of Zinc; and (b) EDAX analysis of force opened region showing only matrix elements.**

0.02 % error in the effective strain is detected. The above two-dimensional model is based on principles of conservation for determining the temperature and stress distribution. Fourier's heat law is used to estimate the heat flux due to the thermal load. This heat flux is essentially related to the temperature gradient. The structural-thermal approach along with thermo-elastic stiffness matrix is employed to estimate resulting stresses.

Homogeneous and isotropic material properties are assumed. Thermal and elastic-plastic properties of material were considered to be temperature dependent. Convection was considered to be the main heat transfer mechanism between the sample and the surrounding. Two different surrounding media namely water and air are considered. It is also assumed that the sides and top surface of the specimen are totally immersed in quenching medium and its bottom surface is exposed only partially. Thus, a lower convective heat transfer coefficient of the bottom surface than the other surfaces is considered. The bottom surface of the specimen is assumed to be stationary i.e. there is no relative motion between the bottom surface and the container. Additionally, the mid-point of the bottom surface is constrained in x-direction.

A transient thermo-mechanical coupled analysis has been carrying-out with Von-Mises yield criterion. A frontal solver has been used with Newton-Raphson iterative method with $L_2$ Norm for both force and displacement load convergence. ANSYS/CAE program has been used for pre and post processing of the data. The results have been captured in multiple time sub-steps for better understanding.

The simulation results obtained for a cylindrical steel pin is presented in Fig. 10 showing stress distribution after different time interval following initiation of quenching in air and water. It can be seen that 300 sec. after quenching the stress is completely tensile in water quenching. The maximum stress is on the surface and is around 1.7 MPa. In contrast, it is tensile on the surface and compressive in the core 300 sec. after air quenching. Further, maximum stress is quite low and equal to 0.2 MPa on the surface. After a time period of 1260

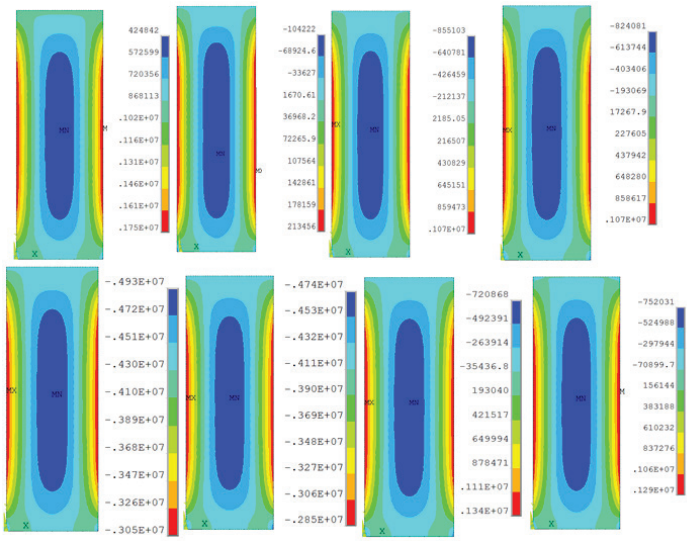

**Figure 10. Simulated stress state in the pin after quenching. Water quenched after (a) 300 s, c; 1260 s, e; 1950 s, g; 3300 s and air quenched after (b) 300 s, d; 1260 s, f; 1950 s, d; 3300 s.**

seconds, stress distribution is similar in both water quenched and air quenched specimen being tensile on the surface and compressive at the interior.

The maximum tensile stress is also around 1 MPa significantly low than initial stage of water quenched sample. 1950 sec. following quenching, the stresses becomes compressive throughout the pin for both water quenched and air quenched pin and the maximum compressive stresses close to 5 MPa is experienced at the core. Finally 3300 sec. after quenching, the surface becomes tensile and the core remains compressive. The differences in stress distribution in water and air quenched sample is reduced. The maximum stresses are also quite low.

## 3. DISCUSSION

The microstructural features and the mechanical properties of the steel pin indicates that the material is used in hardened and tempered condition.. As mentioned earlier, the steel was austenitize at 915 °C, soaked for 65 min. and then water quenched. The steel was then tempered at 485 °C for 65 min. followed by air cooling. During heat treatment of this kind of steel two independent processes take place resulting in generation of residual stresses and distortion. During cooling, in one hand, closely packed fcc austenite transforms to loosely packed bcc ferrite, cementite or bct martensite. This results in expansion of volume.

On the other hand, the pin undergoes normal thermal contraction as the pin is cooled. When the pin is quenched in water from the austenite phase, the near surface region of the pin cools more rapidly than interior. As the austenite transforms near surface region, the volume of the near surface region expands. As long as the temperature is on higher side, the interior accommodate the dimensional changes easily as the untransformed austenite is ductile enough to do so. Gradually interior starts cooling and transforming. The expansion of the interior is constrained by the outer layer which is already hardened and transformed. This results in compression of the interior parts and tension of the surface layer. These stresses are multi-axial[10].

When the pin is cooled in the air following tempering, opposite situation comes into play. Surface layer which cools fast contracts and the hot ductile interior accommodates this contraction. Eventually when interior cools, its contraction is opposed by cooled harder surface layer. This leads to tension in the interior and compression of the outer layer. These stresses which are generated as a result of differential cooling rates of various parts of a component can be high enough to induce non-uniform yielding or plastic deformation during cooling. Even if, yielding does not take place stresses close to yielding stress can remain as residual stress and get superimposed with applied stresses during service. Under certain critical condition, as the situation in the present case, the tensile stress of the surface layer can become high enough to give rise to cracking known as quench cracking instead of yielding. This is what exactly happened in the present case. The fact that crack propagated through intergranular region, supports the contention of quenched cracking.

Simple simulation without taking phase change into consideration indicates change of stress state in the pin is in conformity to the above discussion. Importantly, the maximum tensile stress experienced by the surface during water quenching is significantly higher than that during air quenching in the initial stage of quenching. The high stress state in the surface during water quenching is responsible for initiation of the crack on the surface. The stress state becomes comparable after prolong exposure to quenching medium. This leads to the interference that quenching in the air will be able to prevent crack formation on the surface during quenching. Further since the surface of the pin was threaded, a higher stress gradient is expected resulting in crack initiation.

Oxide layer was noted on the fracture surface. The presence of dark colour oxide layer on the fracture surface, as shown in SEM fractographs (Fig. 7(b)), indicates that the fracture surface has been exposed to high temperatures. This confirms the fact that, crack was initiated before tempering because of the stresses generated during quenching. The intergranular nature of the crack and the presence of oxide layer on the fracture surface suggest that the crack has occurred after quenching and prior to tempering. Fracture surface also revealed presence of Zn. The presence of zinc on the fracture surface till the end of the fracture region confirms that the crack existed prior to the zinc plating.

In view of the above, it is recommended to austenitize the pin in the range of 870-890 °C instead of 915 °C and quench in oil in place of water. Tempering can be done in the range of 480-520 °C followed by oil quenching and not air cooling for this class of material having dimension in range of these pins.

The presence of zinc on the fracture surface gives rise to another possibility known as liquid Zn embrittlement. During this embrittlement, steel becomes brittle and cracks when it comes in contact with molten zinc. Such embrittlement can occur if the strained region comes in contact with liquid zinc. Zn has relatively low melting point and this element is sufficiently mobile. The formation of intermetallic compounds at the interface between the steel and the liquid zinc seems to be responsible for such embrittlement[11]. Zn essentially weakens the grain boundaries resulting in intergranular fracture[12]. However, for failure due to liquid zinc embrittlement to take place, pin needs to be taken to the melting temperature of Zn. It is to be stated that pin was coated with Zn after completion of heat treatment. The pin during testing was not subjected to a temperature where Zn or its intermetallics can melt. Hence failure because of liquid Zn embrittlement is ruled out.

Another possibility is hydrogen embrittlement due to Zinc plating[13]. Zinc electroplating poses a serious problem because of absorption of hydrogen in metals. This leads to hydrogen embrittlement of the substrate and it degrades the mechanical properties of the substrate. It is generally prevented by baking after deposition of zinc on the pin. It is understood that the crack formed before plating of zinc. Hence embrittlement due to hydrogen which comes during zinc plating is not feasible. Another important point is hydrogen embrittlement is generally characterised by concomitant occurrence of intergranular and transgranular fracture[14]. It is also to be stated that the pin was backed after Zn plating to avoid hydrogen embrittlement. Transgranular fracture was not observed in

present investigation. Failure due to hydrogen embrittlement was observed by Slabbert[7], *et al.* and Ifezue and Tobins[8] for conveyor chain pins of a sugar plant and chain anchor pins on a fork lift truck respectively.

At this stage, attempt will be made to examine other possible failure mechanisms. Presence of single cap generally indicates fatigue failure[15]. Presence of striation on facture as noted in case of a component failed by fatigue was not observed. Further, the pin is not subjected to any forms of fatigue stress. Failure due to creep can be a possible reason. In such case, multiple cracks should be seen[16]. This was not observed. Moreover, pin was not exposed to high temperature for sufficiently long time for creep to take place. Failure has not taken place due to abrasive wear[17] or sliding wear[18]. In such cases, delaminating crack characterized by crack propagation parallel to the surface should have been seen[19]. No such crack was noted and on the contrary, observed crack was perpendicular to the surface. Failure due to impact erosion[20] is also ruled out as highly deformed subsurface could not be traced[21.] Moreover, formation of lip and their fracture typical feature of fracture surface of metallic material degraded by impact erosion[22] is also missing.

## 4. CONCLUSIONS

- The pin was made of heat treatable low alloy steel
- The crack was intergranular and the fracture surface was covered with thin oxide layer
- The pin failed because of quench cracking prior to tempering and Zn coating
- Other possible failure mechanisms such as embrittlement due to liquid Zn or hydrogen embrittlement are ruled out.

## REFERENCES


1. Papadopoulou S, Pressas IS, Vazdirvanidis A, Pantazopoulos G. Fatigue failure analysis of roll steel pins from a chain assembly. Fracture mechanism and numerical modeling, Engineering Failure Analysis. 2019; 101, 320–328. doi: 10.1016/j.engfailanal.2019.03.030.
2. Javidinejad A. Full length Ssymmetric versus partial length un-symmetric pin loading failure and analysis for clevis attachments. Journal of Failure Analysis and Prevention. 2016; 16, 67-74. doi: 10.1007/s11668-015-0046-1.
3. Kral MV, Beardsley AL, Breeuwer NJ. Failure analysis of shipping container handler twistlock pin. Journal of Failure Analysis and Prevention, 2020; 20, 641–646. doi: 10.1007/s11668-020-00871-4
4. Xu X, Yu Z. Failure investigation of a diesel engine piston pin. Journal of Failure Analysis and Prevention. 2010; 10, 245-248. doi: 10.1007/s11668-010-9343-x
5. Solazzi L, Mazzù A, Gelfi M. Failure analysis of a cyclic contact testing machine pin. Journal of Failure Analysis and Prevention, 2017; 17, 315-320. doi: 10.1007/s11668-017-0242-2
6. Pepi M, Wechsler G. Failure analysis of horizontal hinge pin components from an army cargo helicopter. Journal of Failure Analysis and Prevention. 2008; 8, 176-182. doi:10.1007/s11668-008-9117-x
7. Slabbert GA, McEwan JJ, Paton R. Failure analysis of carrier chain pins. Engineering Failure Analysis. 1998; 5 (2), 121-128. doi; 10.1016/S1350-6307(98)00009-0
8. Ifezue D, Tobins FH. Failure of chain anchor pins on a fork lift truck. journal of failure analysis and prevention. 2014; 15, 686–690. doi: 10.1007/s11668-015-9995-7
9. Jha AK, Sreekumar K, Mittal MC. Metallurgical studies on a failed EN 19 steel shear pin. Engineering Failure Analysis, 2008; 15, 922–930. doi:10.1016/j.engfailanal.2007.10.006
10. Roy M. Dynamic Hardness of detonation sprayed WC-Co coating. Journal of Thermal Spraying. 2002; 11, 393-399. doi:10.1361/105996302770348790
11. Beal C, Kleber X, Fabregue D, Bouzekri M. Liquid zinc embrittlement of twinning-induced plasticity steel. ScriptaMaterialia, 2012; 66, 1030–1033. doi: 10.1016/j.scriptamat.2011.12.040
12. Bauer KD, Todorova M, Hingerl K, Neugebauer J. A first principles investigation of zinc induced embrittlement at grain boundaries in bcc iron. Acta Materialia. 2015; 90, 69–76. doi:10.1016/j.actamat.2015.02.018
13. Shibayama Y, Hojo T, Koyama M, Akiyama E. Stress-controlled hydrogen embrittlement failure in U-bend high-strength steel. International Journal of Hydrogen Energy. 2024; 88, 1010-1016. doi: 10.1016/j.ijhydene.2024.09.123
14. Li X, Ma X, Zhang J, Akiyama E, Wang Y, Song X. Review of hydrogen embrittlement in metals: Hydrogen diffusion. Hydrogen characterization. Hydrogen Embrittlement Mechanism and Prevention. Acta Metallurgica Sinica. 2020; 33 ,759–773. doi:10.1007/s40195-020-01039-7
15. Madhav S, Roy M. Failure analysis of compressor blades of aero-engine. Journal of Failure Analysis and Prevention. 2022; 22, 968-982. doi: 10.1007/s11668-022-01405-w
16. Madhav S, Roy M. Failure analysis of turbine stator vanes of aero-engine. Engineering Failure Analysis. 2020; 117, 104783. doi: 10.1016/j.engfailanal.2020.104783
17. Roy M, Subba Rao ChV, Srinivas Rao D, Sundararajan G. Abrasive wear behaviour of detonation sprayed WC-Co coatings on mild steel. Surface Engineering. 1999; 15,129-136. doi: 10.1179/026708499101516470
18. Wood RJK, Roy M. Tribology of Thermal-Sprayed Coatings. Surface Engineering for Enhanced Performance against Wear. M. Roy (Ed.), Printforce, the Netherlands. Springer Verlag, Austria. 2013; 1-43. doi: 10.4018/978-1-4666-7489-9
19. Paul SN, Thawari G, David J, Roy M. The influence of precipitation hardening on the reciprocating wear behaviour of metallic materials. Transaction of Indian

Institute of Metal. 2005; 58 , 861-872.
20. Sapate SG, Roy M. Solid particle erosion of thermal sprayed coatings. Therm. Sprayed Coat. Their Tribol. Perform. 2015; 193–226. doi: 10.4018/978-1-4666-7489-9.ch007
21. Roy M, Tirupataiah Y, Sundararajan G. The influence of solid solution and dispersion strengthening mechanisms on the room temperature erosion behaviour of nickel. Materials Science & Technology. 1995; 11, 791-797. doi: 10.1179/mst.1995.11.8.791
22. Roy M. Approaches to enhance elevated temperature erosion resistance of Ni-base super alloys. Materials at High Temperature. 2019; 36(2), 142-156. doi: 10.1080/09603409.2018.1482077

## CONTRIBUTORS

**M. Sai Madhav, Sc C, DMRL** has done his AMIE(MME) from The Institution of Engineers Kolkata and working as a Scientist 'C' at DRDO-DMRL, Hyderabad. He worked on failure analysis of engineering components.
In the current study he involved in conceptualization, methodology, experimental work, report compilation, investigation, data curation, draft report preparation

**Dr Manish Roy, Retd Sc G, DMRL** graduated from IIT, Kharagpur. He retired as a Scientist 'G' from DRDO-DMRL, Hyderabad.
In the present paper he done elemental analysis, report finalization, review, editing, project administration, formal analysis and supervision.